Available online at www.sciencedirect.com

ScienceDirect

Procedia - Social and Behavioral Sciences 96 (2013) 2310 – 2319

Procedia
Social and Behavioral Sciences

13th COTA International Conference of Transportation Professionals (CICTP 2013)

Analysis of Impact of Transverse Slope on Hydroplaning Risk Level

Xin-xin Guo[1*], Chi Zhang[1], Bu-xin Cui[1], Di Wang[1], James Tsai[1]

1.Key Laboratory of Special Area Highway Engineering of Ministry of Education, Chang'an University, Xi'an 710064, Shanxi, China;

Abstract

Hydroplaning has become a major inducement of wet-weather road accidents. By the way of CFD (Computational Fluid Dynamics) approach, this paper frames a finite-element meta-models for rib tires with the rang of different road transverse slopes, aiming to figure out the water pressures on tires under different traveling conditions and to find out the theoretical variational condition and regularities of water pressure of the different parts of the tire tread. Analysis shows that there is not an apparent impact of transverse slope on the action coverage of the high pressure induced by hydrodynamic pressure, but with the increase of the standing water depth, the area of high pressure zone will be larger and the variation is the most apparent when the standing water depth ranges from 5mm to 8mm. Therefore, the consequence of this paper can give recommendations on pavement construction, especially on the construction of drainage.

Keywords: Traffic safety; Transverse Slope; Hydraplaning; Tire-Road- Fluid Model; CFD Approach

1. Introduction

Hydroplaning is in reference to the floating or lift-off of tires forced caused fluid pressure induced by inadequate drainage of the standing water between road surface and the traveling tires. In case of hydroplaning, the tires of a travelling vehicle would be driven by different forces caused by water; the vehicle thus is easier to occur cross slip, and then deviating from its desired trace, which would lead to a decrease of handling stability and an increase of risks of road accidents. Take the nonlinearity of tire material, complexity of fluid flow condition and inelasticity of general experiential equation into consideration, this paper frames a 3-dimensional finite meta-model of rib tires ranging in transverse slopes, and then to figure out the theoretical values and distribution, by way of CFD approach (Fluent), of hydrodynamic pressure in case of different standing water depths and road transverse slopes.

* *Guo Xinxin. Tel.: +84-15249247250; fax: +84-029-62630061.*
E-mail address: 5552058@xnmsn.cn

Selection and peer-review under responsibility of Chinese Overseas Transportation Association (COTA).
doi:10.1016/j.sbspro.2013.08.260

In 1960's, the National Aeronautical and Space Administration (NASA) had made extensive experimental research, through which they developed the well-known NASA equation[1] (1), which has been widely used in the aviation, automobile and pavement engineering fields. The equation says:

$$v_p = 10.35\sqrt{p} \tag{1}$$

Where v_p is the critical hydroplaning speed (in mph; 1mph=1.609km/h) and p is the tire inflation pressure (in psi; 1psi=6.859kPa). In the 21st century, T. F. Fwa and his partners simulated the British pendulum test with ABAQUS (Explicit equation)[2], and they proved that Finite-Element Modeling is practicable as a effective laboratory testing method. Subsequently they framed a 3-dimensional finite meta-model, by Fluent, of acting surface of tire-road-fluid and simulate the model, from which they obtain the impact of tire inflation pressure and tire tread pattern on hydroplaning speed [3, 4, 5].

Currently the development of domestic research on the hydroplaning phenomenon is later and slower. By building a laboratory experiment of rainfall, Ji Tianjian and his partners figured out that the main factors impacting the standing water depth includes intensity of rainfall, road slope, width of subgrade and surface roughness (TD)[6]. Tang Bo-ming and his research group have built the 3-dimensional tire model and fluid dynamics model on wet-weather road by CFD approach. From the simulation and computation by Fluent, they found that with the variation of standing water depth, travel speed, tire tread depth, the tire hydro-dynamic pressure and distribution of water velocity will change dramatically [7].

At present, despite the advances in the hydroplaning phenomenon, Most of researches focus on the impact of characteristics of tire design and fluid, other than road characteristics. However, the design of road cross slope is usually the main measure of road transverse drainage. The past studies on hydroplaning all suppose that the road transverse slope is 0, that is, the studies do not take road characteristics into consideration. But theoretically the road cross slope would have a certain effect on direction of fluid flow, which may affect the distribution of tire hydrodynamic pressure. This paper provides an analysis of the effect of road transverse slope by using the proposed model and CFD approach, and make farther study on the effect on the tire hydrodynamic pressure and distribution of water pressure.

2. Modeling of Tire-Road-Fluid

2.1 Locked Wheel Tire Model

In a stationary observer frame of reference, the hydroplaning phenomenon can be simulated by a wheel sliding along a flooded pavement surface. This paper turns a moving wheel frame of reference for simplification of model, the problem can be modelled as a layer of water and a pavement surface moving at a speed (90km/h) toward the wheel .In either case, a locked wheel is modelled as sliding on a flooded (by water and air) pavement surface. In this study, water is used as a contaminant and the temperature is assumed to be 20°C. Hydroplaning is assumed to occur when the average ground hydrodynamic pressure is equivalent to the tire pressure of the wheel, that is, the vehicle's load is equivalent to the hydrodynamic lift force.

This paper samples Audi A4L TFSI and MichelinP225/55R14 95V respectively as the tested car and tire. The tire load is set to be 4218.3N (430kg), and the tire inflation pressure to be 200kPa.

G.Komandi, a Hungarian scholar, made a series of experiments with different sizes of tire on concrete road, he thus worked out an experimental equation of tire compression δ (cm)[8] (2):

$$\delta = C_1 \frac{F_z^{0.85}}{B_0^{0.7} D^{0.43} p_i^{0.6}} K$$
$$K = 15 \times 10^{-3} \times B + 0.42 \tag{2}$$

Where

δ —— radial tire compression;
C_1 —— parameters related to tire pattern, C_1 =1.15 for diagonal tires； C_1 =1.5 for radial tires;
D —— outer diameter of tire (cm);
B_0 —— breadth of tire tread (cm);
p_i —— tire inflation pressure (100KPa);
F_z —— load of monowheel (daN).

Experiments conducted by Auto Terramechanics Research Room of Jilin University and Changchun Auto Research Institute show that the shape of tire-ground contact area falls in between rectangle and ellipse; it can be found out from the measured contact area that with the lower radial tire compression is, the contact shape is approximate elliptic; while higher radial tire compression turns to be, the contact shape is rectangular with its ends to be curved [8]. In this experiment, the contact area is simplified to be rectangular, for purpose of simplification for numerical analysis. The approximate value of tire-road contact area can be worked out by the following equation [7] (3):

$$A=\left[\frac{\pi}{2}D\left(\frac{\delta}{D}\right)^{s}+\lambda\frac{4-\pi}{4}L_1\right]B_0\left(1-e^{-t\delta}\right)$$
$$B=B_0\left(1-e^{-t\delta}\right) \tag{3}$$

Where

A —— contact area (cm^2);

L_1 —— length of the contact impression when B (breadth of the impression) is $0.95B_0$ (cm);

λ —— constant related with B: $B<0.95B_0, \lambda=0; B\geq 0.95B_0, \lambda=1$;

B —— Breadth of contact impressions of tire-ground (cm).

Tab.1 Value of s and t for the different types of tires

Tire type	5.60R16	5.60-16	5.00-10	4.00-12
Structure type	radial	diagonal	radial	diagonal
Layer number	6	6	4	6
s	0.557	0.553	0.576	0.559
t	122.7	108.9	181.1	113.8

The tire impression and the area of contact impressions thus can be figured out based on the values determined in this experiment:

$$\delta=C_1\frac{F_z^{0.85}}{B_0^{0.7}D^{0.43}p_i^{0.6}}K=\frac{421.83^{0.85}}{22.5^{0.7}\times 65.39^{0.43}\times 2^{0.6}}=1.6cm$$

$$A=\left[\frac{\pi}{2}D\left(\frac{\delta}{D}\right)^{s}+\lambda\frac{4-\pi}{4}L_1\right]B_0\left(1-e^{-t\delta}\right)=\left[\frac{\pi}{2}\times 65.39\times\left(\frac{1.5956}{65.39}\right)^{0.557}+\frac{4-\pi}{4}\times 20.534596\right]\times 22.5=391.3cm^2$$

The transverse slope of road generally is very low (Maximum for 5%), which has few effect on the tire

impression and the area of contact impressions, therefore, the area of contact impressions can be worked out as well as the plane contact area.

2.2 Fluid Flow Model

In this proposed model, the road model is assumed that road surface is smooth. The term "smooth" means that the average roughness height of the micro texture is taken to be 0. The governing equations of fluid flow and the geometrical model for hydroplaning based on the tire deformation model and the pavement surface model are the basis of the numerical model proposed, but complex model of road surface with the diverse roughness height of the micro texture make the numerical model more difficult. Take that into consideration, the average roughness height of the micro texture is taken to be 0 for Simplification of numerical model. As the Navier–Stokes equations are not solvable by simple mathematical methods, the problem is usually solved numerically; this paper thus uses, with Fluent software, the finite volume method, which is adopted for the present study.

2.2.1 Fluid Continuity Equation

The flow in hydroplaning is largely turbulent in nature. This means that any mathematical formulation of hydroplaning must take into account the turbulent nature of fluid flow. In this study, the following Reynolds time-averaged continuity equation (4) is used:

$$\frac{\partial \rho}{\partial t} + \nabla \cdot (\rho V) = 0 \tag{4}$$

Where

ρ = density of the fluid;

v = velocity vector with velocity components *u, v,* and *w i*n the *x, y,* and *z* directions, respectively;

t = time.

2.2.2 Navier-Stokes Momentum Equation

X direction:
$$\frac{\partial(\rho u)}{\partial t} + \nabla \cdot (\rho u V) = -\frac{\partial p}{\partial x} + \frac{\partial \tau_{xx}}{\partial x} + \frac{\partial \tau_{yx}}{\partial y} + \frac{\partial \tau_{zx}}{\partial z} + \rho f_x$$

Y direction:
$$\frac{\partial(\rho v)}{\partial t} + \nabla \cdot (\rho v V) = -\frac{\partial p}{\partial y} + \frac{\partial \tau_{xy}}{\partial x} + \frac{\partial \tau_{yy}}{\partial y} + \frac{\partial \tau_{zy}}{\partial z} + \rho f_y$$

(5)

Z direction:
$$\frac{\partial(\rho w)}{\partial t} + \nabla \cdot (\rho w V) = -\frac{\partial p}{\partial z} + \frac{\partial \tau_{xz}}{\partial x} + \frac{\partial \tau_{yz}}{\partial y} + \frac{\partial \tau_{zz}}{\partial z} + \rho f_z$$

Where τ_{xx}, τ_{yy}, τ_{zz} are shear stresses of fluid components in the x, y, z direction, respectively:

$$\tau_{xx} = \lambda(\nabla \cdot V) + 2\mu \frac{\partial u}{\partial x}$$

$$\tau_{yy} = \lambda(\nabla \cdot V) + 2\mu \frac{\partial u}{\partial y}$$

$$\tau_{zz} = \lambda(\nabla \cdot V) + 2\mu \frac{\partial u}{\partial z}$$

$$\tau_{xy} = \tau_{yx} = \mu\left(\frac{\partial v}{\partial x} + \frac{\partial u}{\partial y}\right)$$

$$\tau_{xz} = \tau_{zx} = \mu\left(\frac{\partial u}{\partial z} + \frac{\partial w}{\partial x}\right)$$

$$\tau_{yz} = \tau_{zy} = \mu\left(\frac{\partial w}{\partial y} + \frac{\partial v}{\partial z}\right)$$

Where μ is the viscosity of the fluid and λ is the second viscosity coefficient:

$$\lambda = -\frac{2}{3}\mu$$

In addition, it is necessary to apply the semi-empirical k–ε model-to-model turbulence of fluid. The RNG k–ε model (6, 7) has been selected to be the modelling of turbulence, which makes small-sized movements are reflected in the large-sized movements and revised viscosity coefficient so as to remove small-sized movements out of the governing equations of fluid flow systematically, which can successfully deal with high strain-rate flow and large bending streamline of fluid:

$$\frac{\partial(\rho k)}{\partial t} + \frac{\partial(\rho k u_i)}{\partial x_i} = \frac{\partial}{\partial x_j}\left[\alpha_k \mu_{eff} \frac{\partial k}{\partial x_j}\right] + G_k + \rho\varepsilon \tag{6}$$

$$\frac{\partial(\rho\varepsilon)}{\partial t} + \frac{\partial(\rho\varepsilon u_i)}{\partial x_i} = \frac{\partial}{\partial x_j}\left[\alpha_\varepsilon \mu_{eff} \frac{\partial \varepsilon}{\partial x_j}\right] + \frac{C_{1\varepsilon}^*\varepsilon}{k} G_k - C_{2\varepsilon}\rho\frac{\varepsilon^2}{k} \tag{7}$$

Where $C_\mu = 0.0845, \alpha_k = \alpha_\varepsilon = 1.39, C_{1\varepsilon} = 1.42, C_{2\varepsilon} = 1.68$

Tab.2 Parameters of the Material Selected for the Model

Parameters / Fluid	Density (kg/m^3)	Dynamic Viscosity (N·s/m^2)	Kinematic Viscosity (m^2/s)
Water	998.2	1.002×10^{-3}	1.004×10^{-6}
Air	1.204	1.82×10^{-5}	1.51×10^{-5}

Note: Air parameter value is measured in standard pressure.

Because of the effect of road surface friction index, the Reynolds Number Re>8000, fluid would be in turbulence. The internal microstructure of turbulence is more complex than laminar flow, in turbulence there are extensive little vortexes moving desultorily, which constantly emerge, develop, attenuation and vanish. These vortexes make the liquid particle mixed with each other, which makes velocity vector of particle, pressure and shear stress etc. of fluid constantly change along with time, thus it is very difficult to simulate and analyse the particles of fluid.

In this paper, interface tracking is achieved through the use of the volume-of-fluid (VOF) model to solve the problem above-mentioned. Through solving a single set of momentum equations and tracking the volume fraction of each of the fluids throughout the domain, VOF model can simulate two or more incompatible fluids, which makes the simulation of every layering of fluid and free surface flow more accurately.

The tracking of the interface between the phases can be accomplished by the solution of the continuity equation for the volume fraction of one or more of the phases. For the *q*th phase, the equation used in Fluent is given as following:

$$\frac{\partial \alpha_q}{\partial t} + u \cdot \nabla \partial_q = 0$$

Where α_q is the volume fraction of *q*th fluid:

$$\sum_{q=1}^{n} \partial_q = 1$$

2.2.3 Boundary Conditions Used

Based on vertical stress and contact impression sizes computed, the area analysed is worked out by multiplying x with z (values of borderlines), thus to be 80×100cm; depth value along the y direction is 5cm, the depth of the inlets for air is to be adjusted with the thickness of ponded water film (see Fig. 1), and the tire tread groove depths are 7mm which stands for general (medium-worn) tire. Tang Boming and his research team [7] point out that despite Fluent can be only workable to acquire mechanical values of fluid under finite-size elements, in fact, when the area to be analysed is large enough, the outcome is approximate to actual values.

For simplifying the model, this paper turns a moving wheel frame of reference for simplification of model; the problem can be modelled as a layer of water and a pavement surface moving at a speed (90km/h) toward the wheel. The schematic diagram of boundary conditions and initial conditions adopted is as shown in Fig.1. The upstream boundary conditions consist of a pair of inlets, namely, a velocity inlet for water and a velocity inlet for air are set in the model. The pavement surface (wall-ground) is modelled as a moving smooth plane wall with no micro texture. The speed of air, water, and the pavement surface is kept at 90 km/h to be consistent possible formation of a bow wave. The side edges and the trailing edge are modelled as pressure outlets, with the pressure set at 0 *k*Pa (i.e., atmospheric pressure). The top boundary is set as a pressure outlet at the atmospheric pressure. Wall-1 and wall-2 are set to be frictionless and the roughness height of a glass surface (K_S) is zero. C_S is chosen to be 0.5 to reflect a roughness structure similar to that of uniform sand grains. The locations of the boundaries

have been chosen such that they would not have any significant effect on the average ground hydrodynamic pressure under the wheel. It's worth noticing that different boundaries conditions may have effect on iterations and convergence.

2.2.4 Description of Mesh Used

Because the size and skewness of the meshes between tire and road surface change greatly, it will be very di fficult to simulate and compute the model when the model meshed with hexahedral meshes. In order to make the computation and simulation more simplified, this paper applies Tet/Hybrid meshes to finite volume model, and r efining meshes between tire and road surface. Four-node tetrahedron elements and six-node wedge elements can make the computation simpler. (See Fig.2)

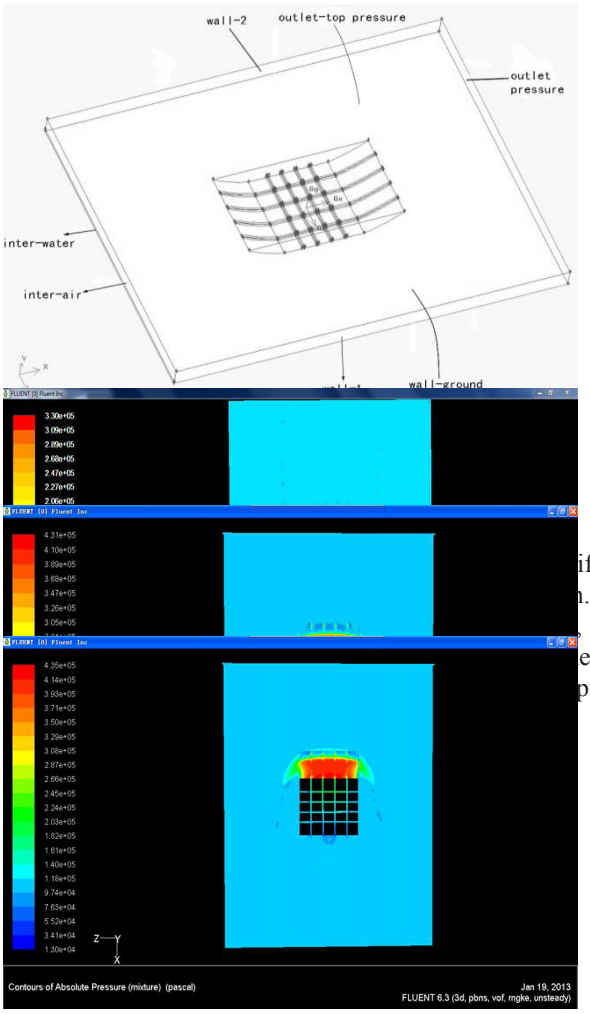

H=12mm，i=0，v=90km/h

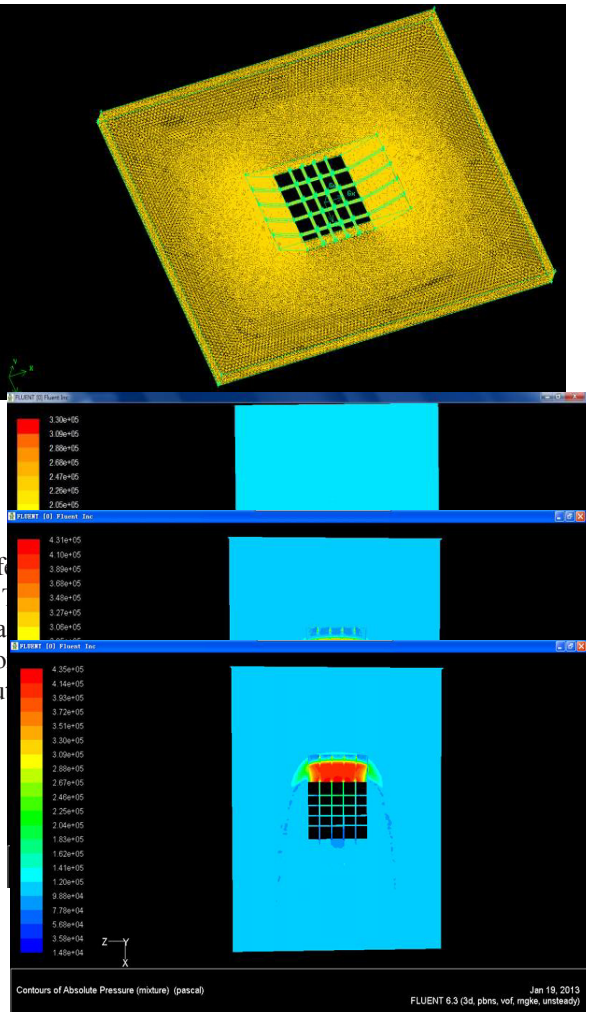

H=12mm，i=2%，v=90km/h

Fig.3 surface-y water pressure distribution (tread groove depths are 7 mm)

3.1 Effect of Standing Water Depth on Hydroplaning

The computing results in Fig.4 show that when traveling velocity is 90km/h, hydro-dynamic pressure of tire will increase along with the thickness of standing water ranging from 5mm to 12mm. When the thickness of standing water is lower than tread groove depth (e.g. 5mm), tire grooves in this case can drain timely, thus the hydro-dynamic pressure of tire is lower than tire inflation pressure; however, with the thickness of water increasing, hydrops gradually emerge in the tread groove, which leads to tire groove isn't able to drain off all water and results in increasing of hydro-dynamic pressure of tire. When hydrodynamic pressure turns to be larger than tire inflation pressure and tires can obtain non-contact with road surfaces, the hydroplaning phenomenon will take place.

The results in Fig.5 show that with the thickness of standing water ranging from 5mm to 12mm, the area of zone of high pressure included in hydro-dynamic pressure of tire will be gradually increasing. According to the computing results (shown in Tab. 3), for a given speed (90km/h), the area of zone of high pressure increased by about 12.4 cm^2 for every 1 mm increase in surface water depth, which makes an increasing amount of tire lie in the zone of high pressure with the thickness of standing water increasing, and the shape of the zone of high pressure turns to be approximate triangular distribution from the middle of tire to the edge.

Tab. 3 Area of high-pressure zone of different transverse slope and water depth

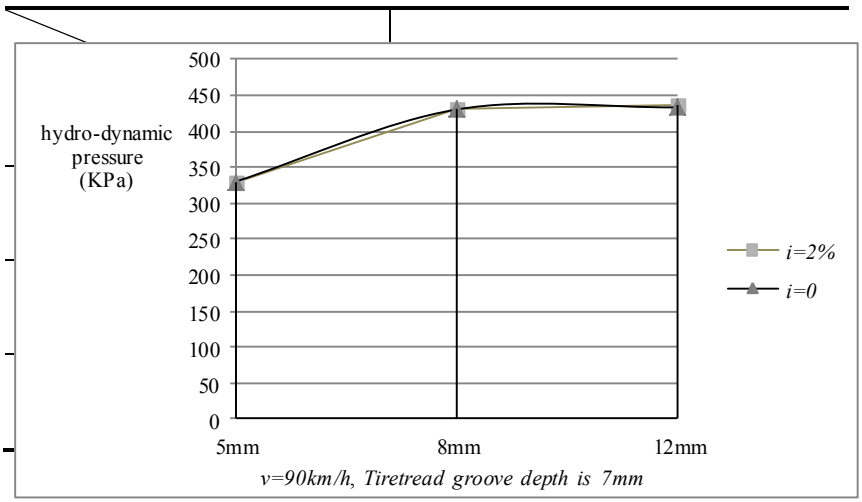

Fig. 4 increasing of hydrodynamic pressure pressure against the thickness of water flow

3.2 Effect of Road Transverse Slope on Hydroplaning

The computing results in Fig.4 and Fig.5 show that for a given speed (90km/h), the transverse slope of road has not apparent effect on distribution of hydrodynamic pressure. Based on the extensive experimental research, Chen Yunhe and his partners point out that the velocity of water on the road is 0.256m/s while the transverse slope of road is 2%, and the longitudinal slope of road is 0. When the thickness of standing water is lower than tread groove depth (e.g. 5mm), tire grooves in this case can drain timely, and the water of cross direction has few

effect on the velocity of tire. However, with the thickness of standing water ranging from 8mm to 12mm, the transverse grooves of tire can't drain off the hydrops timely, which lead to the hydro-dynamic pressure tends to incline as with the flow direction of water (along the Z axis in this paper), and the tendency is more and more apparent as the transverse slope and the thickness of standing water increasing. When the vehicle travels in the deep water (more than 8mm), the hydroplaning phenomenon will occur in the middle of tire, which usually lies abidingly in the zone of high pressure and makes tire move side-to-side and finally causes the decrease of driving stability. The centre high pressure zone of tire will instantly move to the edge of tire when the vehicle turns a corner, and the hydro-dynamic pressure of tire will drop off from one side of tire to another, which makes the distribution of hydro-dynamic pressure be non-uniform and increases the probability of occurrence of hydroplaning.

However, because the impact of velocity of water of cross direction on velocity of tire is very few and the transverse pattern of tire also can drain the most of water of cross direction, generally the influence of transverse slope on hydro-dynamic pressure is few.

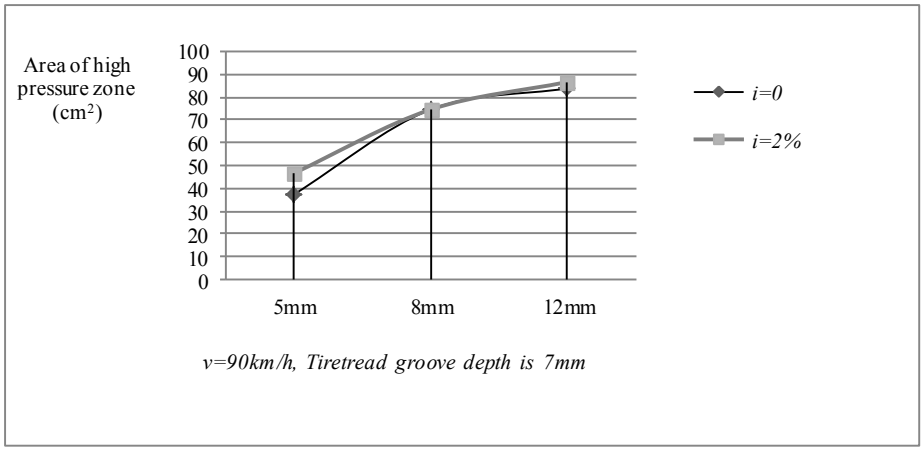

Note: The computing results in this paper is relative high pressure, namely, the area of red pressure zone of tire

Fig. 5 Increase of area of high-pressure zone against the thickness of water flow

4. Conclusion

1) When the vehicle travels at mid or high speed (90 km/h above), the impact of standing water depth on hydrodynamic pressure is very apparent, especially with standing water depth ranging from 5 mm to 8 mm, the increasing rate is the most apparent. Therefore，it is suggested that the car should travel at mid or low speed (65 ~ 85 km/h) on wet-weather road，at the same time highway designing department should pay attention to the design of drainage and maintenance in order to reduce the standing water on the road surface.

2) The results show that when the standing water depth is far less than the tire tread groove depth, the tire tread grooves can completely drain water and the hydroplaning phenomenon don't take place any more, which explains the variation of hydrodynamic pressure is the most apparent when the standing water depth ranges from 5 mm to 8 mm; when standing water depth closes to (or large than) tire tread depth, he tire tread grooves cannot drain off hydrops in the tire grooves completely timely, and the action coverage of the high pressure induced by hydrodynamic pressure will occur in the front of the tire. And with the standing water depth increasing, the area of high-pressure zone will increase markedly. The tire tread groove cannot drain water as original while the tire deviates from the road.

3) The impact of transverse slope of wet-weather road on the hydroplaning safety is not apparent. When the road transverse slope is 2%, the velocity of water of cross direction on the road surface is much lower than the velocity of tire, the tire tread cross grooves can timely drain most of the water of cross direction. In conclusion, with the thickness of standing water ranging from 8mm to 12mm, the hydro-dynamic pressure tends to incline as with the flow direction of water (along the Z axis in this paper), and the tendency is more and more apparent as the transverse slope and the thickness of standing water increasing. But generally the influence of transverse slope on hydrodynamic pressure is few.

Acknowledgements

The project was supported by the Special Fund for Basic Scientific Research of Central Colleges, Chang'an University (No.CHD2012JC091 and CHD2012TD008), the Doctoral Fund of Ministry of Education of China (20120205120013), the Shaanxi Natural Science Funds (NO. 2012JQ7001) and supported by Program for Innovative Research Team in University (NO. IRT1050).

References

[1]. Horne, W. B., and T. J. W. Leland. Influence of Tire Tread Pattern and Runway Surface Condition on Braking Friction and Rolling Resistance of a Modern Aircraft Tire [J]. NASA TN D-1376. National Aeronautics and Space Administration, 1962.

[2]. Yurong Liu, T. F. Fwa, M.ASCE，Y. S. Choo. Finite-Element Modeling of Skid Resistance Test [J]. Journal of Transportation Engineering. ASCE, 2003.5

[3]. G. P. Ong, T. F. Fwa, J. Guo. Modeling Hydroplaning and Effects of Pavement Microtexture [J]. Journal of the Transportation Research Board, No. 1905, Transportation Research Board of the National Academies, Washington.D.C. 2005, pp.166-176

[4]. G. P. Ong, T. F. Fwa. Analysis of Effectiveness of Longitudinal Grooving Against Hydroplaning [J]. Journal of the Transportation Research Board, No. 1949, Transportation Research Board of the National Academies, Washington,D.C,2006, pp. 113-125.

[5]. G. P. Ong, T. F. Fwa. Transverse Pavement Grooving against Hydroplaning [J]. Journal of Transportation Engineering. Vol. 132,No. 6, June 1, 2006.

[6]. G. P. Ong, T. F. Fwa. Effectiveness of Transverse and Longitudinal Pavement Grooving in Wet-Skidding Control [J]. Journal of the Transportation Research Board, No. 2005. Transportation Research Board of the National Academies, Washington D.C.. 2007, pp. 172-182.

[7]. Liu Tangzhi, Tang Boming, Dong Bin, Gao Jianping. Analysis of Impact of Tire Tread Groove Depth on Hydroplaning Risk Level [C]. CIVS.

[8]. Zhuang Jide. *Automobile Tire Theory* [M]. Beijing: Beijing Institute of Technology Press. 1999

[9]. Chen Yunhe, Qian Guochao, Li zhigang. Calculations of Free Water Drainage Current Velocities over Pavement and Slope [J]. Journal of Highway and Transportation Research and Development. 2003, 20(5).